Nanoscale

Accepted Manuscript

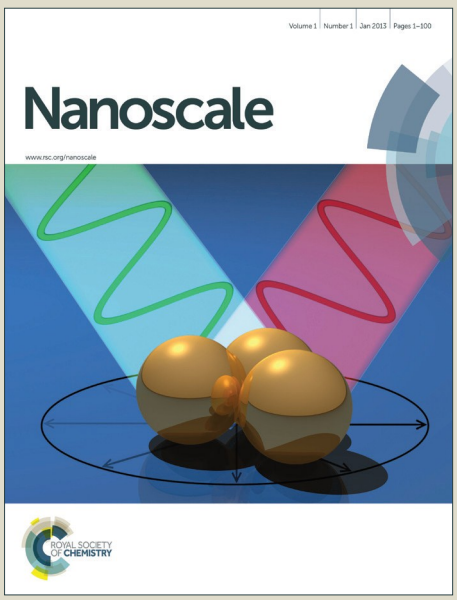

ROYAL SOCIETY OF CHEMISTRY

www.rsc.org/nanoscale

Understanding Carbon-Monoxide Oxidation Mechanism on Ultrathin Palladium Nanowire: The Density Functional Theory Study

Po-Yu Yang[1], Shin-Pon Ju[1,2,*], Zhu-Min Lai[1], Jenn-Sen Lin[3] and Jin-Yuan Hsieh[4]

[1]Department of Mechanical and Electro-Mechanical Engineering, National Sun Yat-sen University, Kaohsiung 804, Taiwan

[2]Department of Medicinal and Applied Chemistry, Kaohsiung Medical University, Kaohsiung 807, Taiwan

[3]Department of Mechanical Engineering, National United University, Miaoli 360, Taiwan

[4]Department of Mechanical Engineering, Minghsin University of Science and Technology, Hsinchu 304, Taiwan

Abstract

The CO oxidation mechanism catalyzed by the ultrathin helical palladium nanowire (PdNW) was investigated by the density functional theory (DFT) calculation. The helical PdNW structure was constructed on the basis of simulated annealing basin-hopping method (SABH) with the tight-binding potential and the penalty method in our previous studies (J. Mater. Chem., Vol. 22, pp 20319, 2012). The low-lying adsorption configurations as well as the adsorption energies for O_2 and CO molecules on different PdNW adsorption sites were obtained by the DFT calculation. The most stable adsorption configurations for the Langmuir-Hinshelwood (LH) mechanism processes were considered for investigating the CO oxidation mechanism. The nudged elastic band (NEB) method was adopted to obtain the transition state configuration and the minimum energy pathways (MEPs).

Keywords: Palladium Nanowire, Basin-Hopping Method, Tight-Binding Potential, Nudged Elastic Band Method.

I. Introduction

The carbon monoxide (CO) is a colorless, odorless, and very toxic gas for humans due to its high affinity with hemoglobin. Carbon monoxide can be generated in various natural and artificial environments, especial exhaust from cars and factories. Consequently, the catalytic conversion developed in 1970s is the important CO elimination treatment. The main depollution process of the conversion is the CO oxidation, which is usually catalyzed by the noble metals (Pt, Pd, Rh) for transforming CO into CO_2[1, 2].

In platinum (Pt)-based catalysts, the strong interaction between active sites and CO molecules may cause serious activity loose, which is called CO poisoning[3, 4]. Thus, Palladium (Pd) has been considered as the replacement material because the Pd material is abundant and inexpensive as well as the higher CO endurance than that of Pt materials. In addition, Pd materials have the similar catalytic behavior with Pt, but display more long-term durability in acidic media. The studies of CO oxidation mechanism are very important and have attracted the intensive attention of researchers. For instance, Andreas Eichler used the DFT calculation to simulate the CO oxidation mechanism on the transition metal surface[5]. Yanhui Zhang *et al*. investigated the effect of different Pd oxidation states on the catalytic activity of CO oxidation[6]. Wei Zhang *et al.* used the DFT calculation to observe the catalytic efficiency of CO oxidation on Au-Pd bimetallic clusters[7-10]. William *et al*. studied the effect of Pd cluster size on the catalytic efficiency of Pd for the CO oxidation reaction[11].

Since the development of nanotechnology, the nanostructure of transition metals have been studied and applied to the catalysis field. For examples, ultrathin Pt nanowires with the diameter about 1.8nm have been synthesized and used in the electrocatalytical application for hydrogen evolution reaction[12]. Core-shell

nanoparticles of metal oxide/noble metal have also been fabricated and applied to the CO oxidation reaction[13, 14]. One-dimensional nanowires have been widely used in the catalytic application and are accessible in experimental manufacturing process. Although many previous studies have reported the CO oxidation catalytic mechanism by the nanomaterials, the study about the CO oxidation mechanism on the Pd nanowire is still lack. In this work, the investigation of CO oxidation catalyzed by the ultrathin Pd nanowire was studied. The DFT calculation was employed to figure out the active sites on the Pd nanowire as well as the search for the minimum energy pathways (MEPs) of the catalytic mechanism.

II. Simulation Model

The structure of ultrathin palladium (Pd) nanowire was constructed by the simulated annealing basin-hopping method (SABH), which can be seen in our previous studies[15, 16]. The density functional theory (DFT) implemented by $Dmol_3$ package[17, 18] was used to obtain all optimized configurations and their electronic properties for the catalytic process. The spin-unrestricted DFT in the generalized gradient approximation (GGA) with the Perdew−Wang exchange and correlation functional (PW91) was adopted[19]. The basis set was the effective core potential (ECP) and a double numerical level including a d-polarization function (DND).

The adsorptions of carbon monoxide (CO) and oxygen molecule (O_2) on different sites of Pd nanowire were considered. The adsorption energy is defined as:

$$E_{ads} = E_T[nanowire + X] - (E_T[nanowure] + E_T[X]) \quad (1)$$

where the $E_T[nanowire + X]$ is the total energy of adsorbed X (O_2 or CO) with the Pd nanowire, $E_T[nanowure]$ is the energy of Pd nanowire, $E_T[X]$ is the energy of adsorbate X in gas phase. In addition, the MEPs for catalytic reactions and

configurations of transition states were determined by the nudged elastic band (NEB) method[20].

III. Result and discussion

Figure 1(a) and 1(b) show the top view and side view of PdNW unit cell, comprising of 44 atoms, and the length of the unit cell along the axial direction is 27.77 Å after optimization by DFT calculations. Figure 1 (c) represents that atoms in the chains marked in yellow form a relatively flat surface, which are designated as flat convex Pd atoms, Pd_f. The dark green atoms in the chains form a local sharp convex structure with the helical atom chain. Consequently, these atoms are labelled as sharp convex Pd atoms, Pd_s. Fig. 1(d) shows the cross section of the PdNW, and the distances between two Pd_s atoms (d_{ss}) of different chains and between two Pd_f atoms (d_{ff}), representing cross-sectional length, of different chains are 4.38 Å and 2.92 Å, respectively, indicating the cross section of H-wire is not circular.

For convenience to present our DFT results, three types of adsorption sites including top, bridge and hollow were defined as shown in Figure 2. The top site (T) is one atom or molecular adsorbed on the single Pd atom, the top sites on the flat chain are designated as T1, while those on the sharp chain are designated as T2; The bridge site (B) is the adsorbate bound between two nearest Pd atoms. According to the types of Pd-Pd bonding, we can divide these bridge sites into B1, B2, and B3 sites; The hollow site (H) is the adsorbate locate in the middle space around three Pd atoms, and H1 and H2 are also considered by different Pd arrangements. For obtaining the most probable reaction site of CO oxidation on the Pd nanowire, the adsorption energies of O_2 and CO on the Pd nanowire with different adsorption sites are performed by DFT calculations. The results of adsorption energies are listed in Table 1. For the adsorption of an oxygen molecule, two configurations were concerned. The

end-on form is defined as the O-O double bond perpendicular to the axis of the Pd nanowire and the O-O double bond is parallel to the nanowire axis in the side-on form. For all adsorption sites, the CO molecule presents much higher adsorption energies than those of O_2. In addition, B3 sites display the highest adsorption energies for both O_2 or CO, indicating the B3 site is the most active site for CO oxidation on the Pd nanowire.

For the bimolecular reaction on surfaces, there are two kinds of mechanisms, Eley-Rideal (ER) and Langmuir-Hinshelwood (LH). The previous experimental study[21] and the theoretical study[22] show that the CO oxidation on typical transition-metal surface prefers to the LH mechanism. Therefore, the system of the pre-adsorbate CO on the B3 site was considered for the LH mechanism. The schematic reaction pathway with the corresponding potential energies is shown in Figure 3. For the MEP of CO oxidation, the configuration of an O_2 molecule co-adsorbed with the pre-adsorbed CO was used as the reactant configuration. Next, the neighboring CO and O2 molecules pass over the first transition state (TS1) with the energy barrier of 0.73 eV. The peroxo-type O-O-C-O intermediate forms, which is 0.34 eV lower than that of TS1. The O-O bond length is elongated from 1.515 Å to 1.695 Å to reach the second transition state (TS2) with the lower energy barrier by 0.07 eV. Finally, desorption of CO_2 molecule occurs and an O atom is left on the Pd nanowire. The total reaction energy of CO oxidation on the Pd nanowire was -4.53 eV, which exhibits the exothermic process. Since the end-on O_2 molecule at the B_3 site possesses the highest adsorption energy as shown in Table 1, the migration of an O_2 molecule from B3 site to B1 site could be the rate determining step for the MEP shown in Figure 3. By the NEB method, the predicted barrier is about 1.62 eV, which is much higher than the energy barrier for TS1 by 0.89 eV. It indicates the migration of an O_2 molecule from B3 site to B1 site is the rate determining step for the CO

oxidation. From the experimental results of Chen's study[23], the CO oxidation efficiency on the Pd surface can be significantly enhanced by increasing the O_2/CO ratio. It implies the CO oxidation may begin with the O_2 configuration adsorbed directly from the gas phase instead of those after the migration from a stronger adsorption site. Accordingly, the MEP shown in Figure 3 is significant for the Pd nanowire at a certain O_2/CO ratio.

The reaction pathway of the second CO oxidation with wire-O was further calculated and the schematic reaction pathway is shown in Figure 4. For the MEP of second CO oxidation, the O atom was located at the B1 site, which is identical to the last wire-O configuration of the first CO oxidation MEP in Figure 3. Following the LH mechanism, the CO adsorbed on the most stable B3 site passes over the first transition state with the energy barrier of 1.40 eV and then reaches a stable wire+OCO intermediate. Finally, the intermediate passes over a small barrier of 0.32 eV and the CO is oxidized to CO2.

For comparison of the second CO oxidation barrier with those of low miller index facets, the CO oxidation by the O atom on the Pd(100) and Pd(111) were considered by following the CO and O adsorption sites in Eichler's study5. In the simulations of Pd(100) and Pd(111) surfaces, the p(2 × 3) lateral cells were used and the coverage effect on the calculated stability of adsorption energies is negligible (smaller than 0.1 eV). The p(2 × 3) lateral cells of the Pd(100) and Pd(111) surfaces were modeled as the periodically repeated slabs with 4 layers. The bottom two atomic layers were kept frozen and set to the experimentally estimated bulk parameters, and the remaining layers were fully relaxed during the calculations. The lateral cells have dimensions of a = 11.67 Å, b = 7.80 Å, and c = 20.84 Å for Pd(100) surface and dimensions of a = 11.04 Å, b = 8.28 Å, and c = 21.76 Å for Pd(111) surface. Both simulation boxes include a vacuum region of thickness 15 Å upon, which guarantees

no interactions between the upper and lower slabs of the Pd(100) and Pd(111) substrates. Table 2 lists the calculation results of current studies and those of Eichler's study for Pd(100) and Pd(111) surfaces as well as the barriers of the first CO oxidation by Pd nanoclusters and the nanowire of current study. For the Pd(100) and Pd(111) surfaces, the barriers of the second CO oxidation are about 0.95 eV and 1.29 eV, which are close to those of Eichler's study and are lower than that of Pd nanowire by 0.45 eV and 0.11 eV. For the first CO oxidation, one can see the barriers of Pd13 and Pd38 are close to that of Pd nanowire.

IV. Conclusions

In this work, the CO oxidation mechanism has been investigated by the DFT calculations. According to the adsorption energy calculations, the O_2 and CO were adsorbed on top, bridge, and hollow sites. The results indicate B3 site is the most stable site on the Pd nanowire for pre-adsorbed CO molecule. Furthermore, the energy barrier of CO oxidation for the LH reaction is lower than those on Pd bulk surfaces, indicating the better catalytic efficiency of Pd nanowire. Although the adsorption energies of CO are 0.4-0.6 eV higher than those of O_2 on the Pd nanowire as shown in Table 1, the CO poisoning can still be avoided by increasing the O_2/CO ratio to reach the hyperactive states, at which the reaction probabilities of CO molecules almost approach unity[23]. In the current DFT model, although we cannot provide the direct calculation results about how much the partial pressure of O2 could change the CO adsorption preference, the adsorption energies listed in Table 1 can be used to obtain the adsorption probabilities of an O2 molecule or a CO molecule on different sites of Pd nanowire by using the Arrhenius equation. For considering the adsorption probability from the gaseous CO/O2 mixture, the collision frequency24 of CO and O2 molecules with the Pd nanowire surface should be concerned. According to Chen's

study, the hyperactive state of Pd surface may occur as the O2/CO ratio exceeds 11 at 550 K. It implies the increase in the O2/CO ratio could increase the O2 collision frequency with the Pd surface and change the CO adsorption preference. Table 3 shows the strongest adsorption energies of Pd(100), Pd(111), and Pd nanowire for CO and O2. The adsorption energy differences between CO and O2 on Pd nanowire, Pd(100) and Pd(111) are 1.14 eV, 1.44 eV and 1.66 eV, respectively. Because the adsorption energy difference of Pd nanowire is the smallest, it indicates the CO poisoning could be less significant for the CO oxidation by the Pd nanowire and the hyperactive state could achieve by a lower O2/CO ratio for the Pd nanowire surface.

References

1. D. I. Enache, J. K. Edwards, P. Landon, B. Solsona-Espriu, A. F. Carley, A. A. Herzing, M. Watanabe, C. J. Kiely, D. W. Knight and G. J. Hutchings, *Science*, 2006, 311, 362-365.
2. T. Bunluesin, R. Gorte and G. Graham, *Applied Catalysis B: Environmental*, 1998, 15, 107-114.
3. A. Bourane and D. Bianchi, *Journal of Catalysis*, 2004, 222, 499-510.
4. A. Bourane and D. Bianchi, *journal of Catalysis*, 2001, 202, 34-44.
5. A. Eichler, *Surface science*, 2002, 498, 314-320.
6. Y. Zhang, Y. Cai, Y. Guo, H. Wang, L. Wang, Y. Lou, Y. Guo, G. Lu and Y. Wang, *Catalysis Science & Technology*, 2014, 4, 3973-3980.
7. S.-L. Peng, L.-Y. Gan, R.-Y. Tian and Y.-J. Zhao, *Computational and Theoretical Chemistry*, 2011, 977, 62-68.
8. H.-L. Chen, C.-H. Su and H.-T. Chen, *Chemical Physics Letters*, 2012, 536, 100-103.
9. W. Zhang, D. Cheng and J. Zhu, *RSC Advances*, 2014, 4, 42554-42561.
10. R. W. Scott, C. Sivadinarayana, O. M. Wilson, Z. Yan, D. W. Goodman and R. M. Crooks, *Journal of the American Chemical Society*, 2005, 127, 1380-1381.
11. W. E. Kaden, W. A. Kunkel, M. D. Kane, F. S. Roberts and S. L. Anderson, *Journal of the American Chemical Society*, 2010, 132, 13097-13099.
12. H. Yin, S. Zhao, K. Zhao, A. Muqsit, H. Tang, L. Chang, H. Zhao, Y. Gao and Z. Tang, *Nature communications*, 2015, 6, 6430.
13. J. Chen, D. Wang, J. Qi, G. Li, F. Zheng, S. Li, H. Zhao and Z. Tang, *Small*, 2015, 11, 420-425.
14. J. Qi, J. Chen, G. Li, S. Li, Y. Gao and Z. Tang, *Energy & Environmental Science*, 2012, 5, 8937-8941.
15. K.-H. Lin, S.-P. Ju, H.-L. Chen, H.-T. Chen, M.-H. Weng, J.-S. Lin, J.-Y. Hsieh, H.-W. Yang and W.-C. Huang, *Journal of nanoscience and nanotechnology*, 2013, 13, 813-818.
16. S.-P. Ju, M.-H. Weng and W.-C. Huang, *Journal of Materials Chemistry*, 2012, 22, 20319-20333.
17. B. Delley, *The Journal of chemical physics*, 1990, 92, 508-517.
18. B. Delley, *The Journal of chemical physics*, 2000, 113, 7756-7764.
19. J. P. Perdew and Y. Wang, *Physical Review B*, 1992, 45, 13244.
20. A. Ulitsky and R. Elber, *The Journal of chemical physics*, 1990, 92, 1510-1511.
21. T. Engel and G. Ertl, *The Journal of Chemical Physics*, 1978, 69, 1267-1281.
22. H. C. Ham, J. A. Stephens, G. S. Hwang, J. Han, S. W. Nam and T. H. Lim, *The Journal of Physical Chemistry Letters*, 2012, 3, 566-570.
23. M. Chen, Y. Cai, Z. Yan, K. Gath, S. Axnanda and D. W. Goodman, *Surface Science*, 2007, 601, 5326-5331.
24. A. Farkas, F. Hess and H. Over, *The Journal of Physical Chemistry C*, 2011, 116, 581-591.

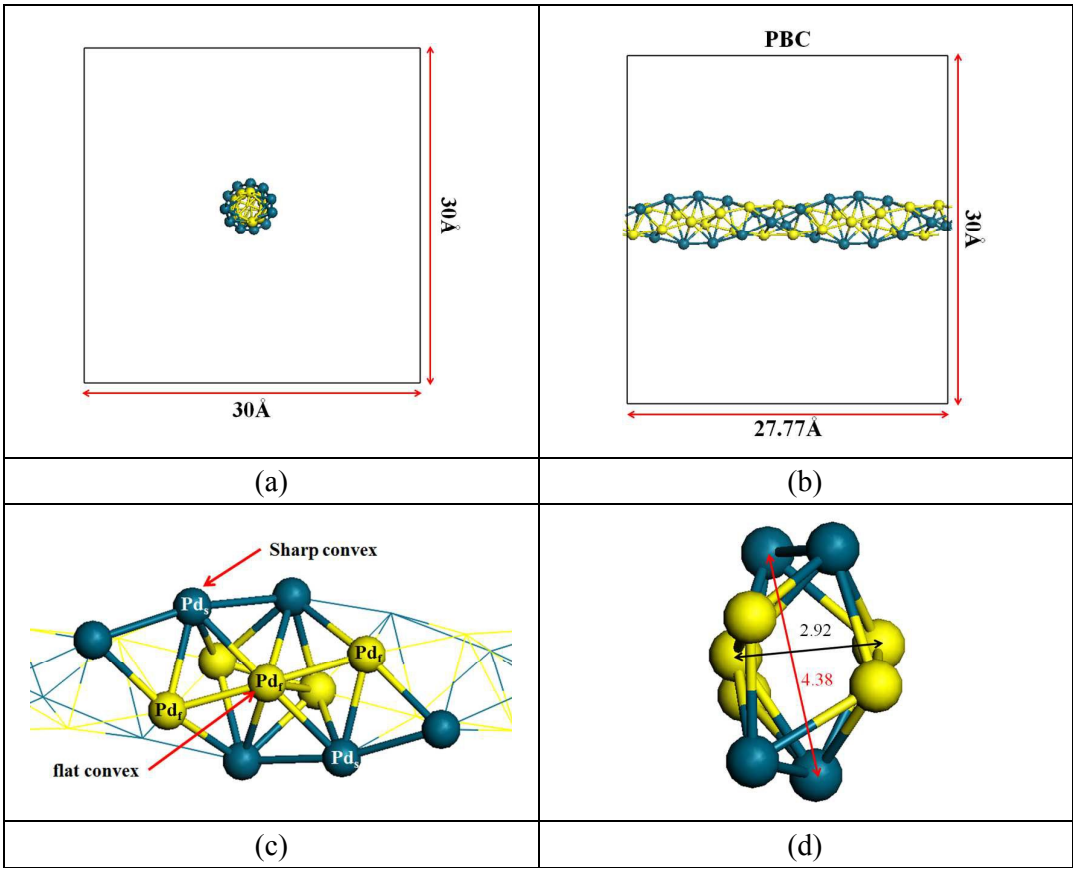

Figure 1 Schematic diagram of Pd helical nanowire (a) top view, (b) side view, (c) local side view, and (d) the bond lengths d_{ss} (red) and d_{ff} (black)

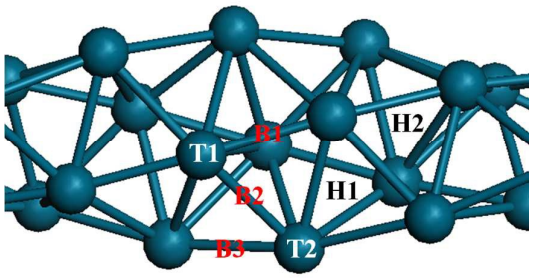

Figure 2 The labels T, B and H represent top, bridge, and hollow sites. Note that T type is the adsorbate binding with single Pd atom, B type is the adsorbate binding with two Pd atoms as bridge, and H type is the adsorbate locate in the hollow which surrounded by three Pd atoms.

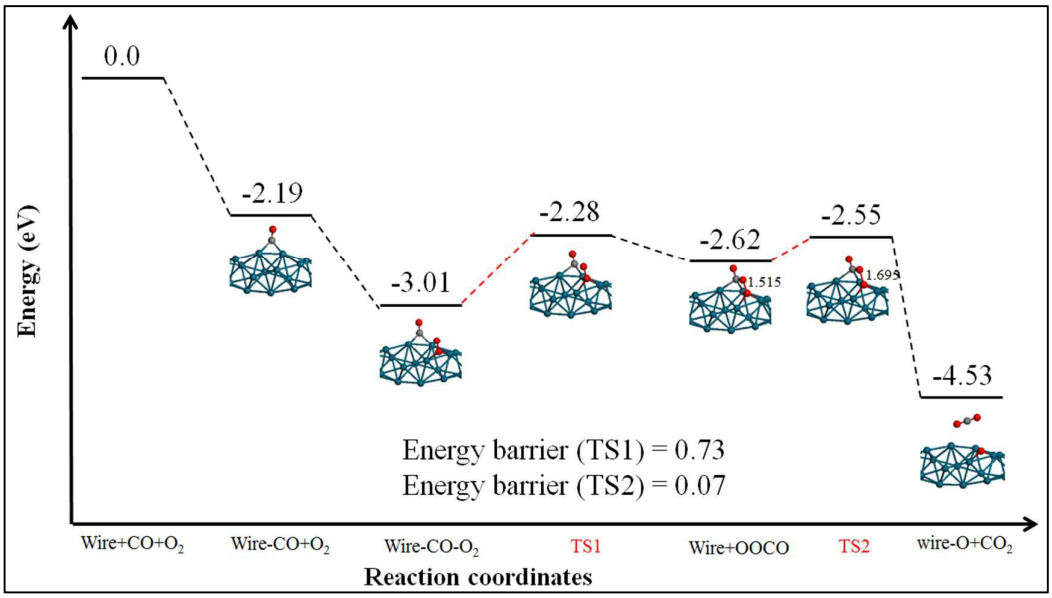

Figure 3 Schematic potential energy profile of first CO oxidation with LH reaction pathway on Pd nanowire.

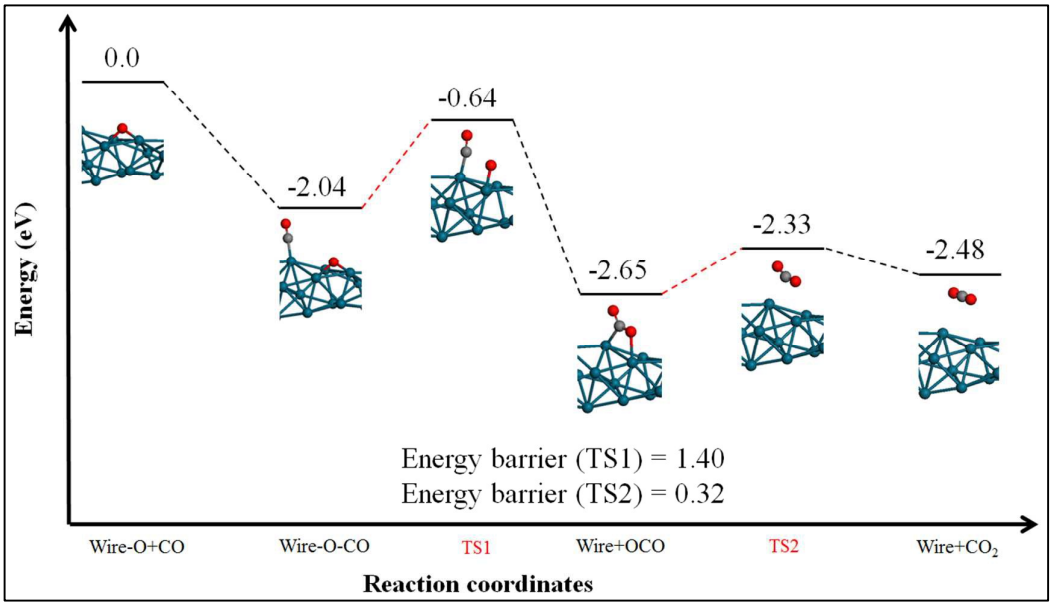

Figure 4 Schematic potential energy profile of second CO oxidation with LH reaction pathway on Pd wire-O.

Table 1 The adsorption energies of CO and O_2 adsorbed on the Pd nanowire. (U means unstable)

Adsorbate : O_2 (end on)		**Adsorbate : O_2 (side on)**		**Adsorbate : CO**	
position	**Adsorption energy (eV)**	**position**	**Adsorption energy (eV)**	**position**	**Adsorption energy (eV)**
H1	U	**H1**	U	**H1**	-2.07
H2	U	**H2**	U	**H2**	-1.98
B1	-0.57	**B1**	-1.43	**B1**	-2.04
B2	U	**B2**	-1.35	**B2**	-1.95
B3	-1.06	**B3**	-1.74	**B3**	-2.20
T1	-0.71	**T1**	U	**T1**	-1.67
T2	-0.90	**T2**	U	**T2**	-1.85

Table 2 The relative energies of initial state, transition state, and the energy barriers on different Pd catalysts.

	Pd(100)	Pd(111)	Pd_{13} cluster	Pd_{38} cluster	Pd nanowire	
mode	CO + Pd-O		CO + Pd-O_2		CO + Pd-O_2	CO + Pd-O
$E_{Barrier}$ (eV)	1.05[a] 0.95[d]	1.40[a] 1.29[d]	0.81[b]	0.59[c]	0.73[d]	1.40[d]

a. A. Eichler, Surface science, 2002, 498, 314-320.
b. W. Zhang, D. Cheng and J. Zhu, RSC Advances, 2014, 4, 42554-42561.
c. H.-L. Chen, C.-H. Su and H.-T. Chen, Chemical Physics Letters, 2012, 536, 100-103.
d. This work.

Table 3 The difference of adsorption energies between CO and O_2 on the Pd nanowire, Pd(100) and Pd(111). The letter in the parentheses indicates the strongest adsorption site of CO or O_2 on these surfaces.

Adsorption energy (eV)	Pd(100)	Pd(111)	Pd nanowire
$E_{ads, CO}$	-1.97 (B)	-1.81 (B)	-2.20 (B3)
$E_{ads, O2 (end on)}$	-0.53 (T)	-0.15 (B)	-1.06 (B3)
ΔE ($E_{ads, O2}$ - $E_{ads, CO}$)	1.44	1.66	1.14